

Acoustic interferometry for sediment geoaoustic characterization using broadband ship noise in the Yellow Shark environment

Qun-yan Ren, Jean-Pierre Hermand, and Sheng-chun Piao

I. INTRODUCTION

For accurate sound propagation prediction and sonar applications in shallow water, the environmental properties, especially for the ocean bottom are required. To estimate the ocean bottom geoaoustic properties, many techniques, e.g., direct measurements [1], nonlinear inversion methods [2-5] and analytical adjoint models [6] are developed. In these applications, the controlled and high power source is usually employed. However, this can result in high maintenance cost, not applicable in all situations and may harm the marine animals. In this paper, an acoustic passive interferometry technique for sediment geoaoustic characterization by processing the noise of a passing surface ship is introduced.

Spectrogram of broadband sound field radiated by a moving source usually exhibits interference structure in the form of striations in the time-frequency or equivalent space-frequency plane. Its structure is determined by the parameters that characterize the acoustic propagation medium. Waveguide invariant theory [7] provides an interpretation of the interference phenomenon and has been applied in underwater inverse problems. Here, a passive acoustic interferometry technique is proposed for sediment geoaoustic characterization using a set of striation locations extracted by a multi-scale line filter. A synthetic test for sediment geoaoustic characterization using the relationship in acoustic interferometry technique based on the Yellow Shark environmental model is given. Finally, preliminary results of using acoustic data due to passing ships collected in Mediterranean Sea in 2007 are presented.

II. ACOUSTIC INTERFEROMETRY TECHNIQUE

According to normal mode theory, for a hypthetic environment E_0 , the sound intensity I generated by a point omni-directional source of circular frequency ω at depth z_0 , received at range r_0 and depth z can be expressed as [8]:

$$I \approx \frac{1}{r} \sum_l B_l^2 + \frac{1}{r} \sum_{l,m(l \neq m)} B_l B_m^* \cos(\Delta \xi_{l,m} r) \quad (1)$$

where $B_l = \sqrt{2\pi/k_l} \phi_l(z_0) \psi_l(z)$, and ϕ_l and ξ_l are the modal function and eigenvalue for mode l , respectively. $\Delta \xi_{l,m} = \xi_l - \xi_m$ and $*$ denotes for complex conjugate. In the vicinity of a local extreme [9]:

$$\Delta I = \frac{\partial I}{\partial \omega} \Delta \omega + \frac{\partial I}{\partial E} \Delta E = 0 \quad (2)$$

Suppose the modal function changes with frequency and environmental perturbation much more slowly than the phase, in the linear approximation and assumption that each parameter are independent, the relation between the frequency shift and environmental perturbation can be approximate as [10]:

$$\Delta \omega \equiv k \Delta x \quad (3)$$

where k is determined by the environmental property, once it is known, the environmental properties can be inverted by measuring the frequency shift compared to a reference environment.

Qun-yan Ren is currently a PhD student at the Environmental Hydroacoustics Laboratory (EHL), Faculty of Applied Science, Université libre de Bruxelles (U.L.B.), Belgium, in co-tutelle with the National Key Laboratory of Underwater Acoustic Technology, Harbin Engineering University (HEU), China (phone: +32-(0)2-650.67.69; e-mail: qunyanren@ulb.ac.be).

Jean-Pierre Hermand is with the EHL, Faculty of Applied Science, U.L.B., Belgium (e-mail: jhermand@ulb.ac.be).

Sheng-chun Piao is with National Key Laboratory of Underwater Acoustic Technology, HEU, China (e-mail: piaoshengchun@ulb.ac.be).

However, there can be many parameters to characterize the sediment. Rather than inverting for all these parameters at once, the method proposed here is to estimate first the main parameters that affect the sound propagation with the following steps:

1. Find the critical sediment geoacoustic parameters that affect broadband sound field;
2. Reveal and interpret the relation between the striation shift and main sediment geoacoustic parameter perturbation;
3. Estimate the critical parameters using the revealed relation.

By numerical simulations [11], the sediment layer thickness and compression sound speed are found to have significant effects on the striation position for the Yellow Shark environmental model [12]. In this paper, the passive acoustic interferometry technique uses a set of striation locations extracted by the multi-scale line filter [13] for the rapid characterization of sediment thickness and sound speed. As revealed in [10], the relation between frequency shift and these two parameter perturbations (compared with a reference sediment layer) can be interpreted as:

$$\Delta f = a\Delta C_p + b\Delta H + c\Delta C_p\Delta H + d \quad (4)$$

a, b, c and d are constants for specific striation and determined by fitting ambiguity functions in a least-square sense. Once these parameters are known, then one can use the following equation to estimate the sediment thickness and sound speed.

$$|\Delta f_{pre} - \Delta f_{mea}| \leq err \quad (5)$$

where err is the precision. An example of using striation L2 and R2 in Fig. 1 is presented in [10].

While for the broadband sound distribution of a passive ship, because of non-flat of source spectrogram and the complexity of propagation medium, the striations are usually non-continuous. The clearly visible striations in real data may not exactly correspond to that of numerical simulations. Consequently, the derived constants for specific striation of the synthetic data may not apply to that of real data. It is better for one to have an idea of the average constants for a certain range interval and frequency band, and then uses them to estimate the preliminary estimation for the sediment property with more flexibility when processing real data. Here, another two striations in yellow box denoted as striation L1 and R1 are selected, following the same steps as that of [10], one can get their constants and then finally get the average value for these four striations: $a = 0.0093$, $b = -1.8908$, $c = 0.0204$ and $d = 0.2903$. In this paper, the using of the average constants of the four striations is examined.

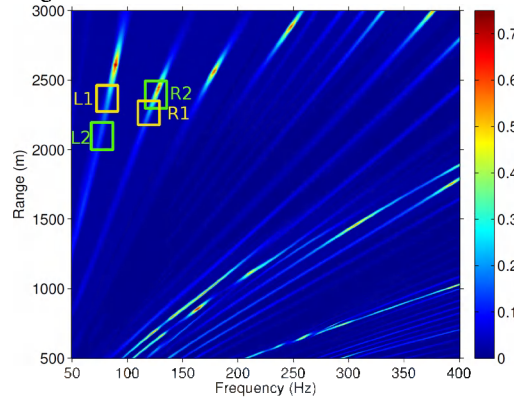


Figure 1: Calculated line structure of the space-frequency distribution of the broadband sound intensity (in dB) for a reference sediment with thickness of 0.5 m and sound speed of 1460 m/s.

III. NUMERICAL TEST

Assume a sediment layer has a thickness of 6.5-m and sound speed of 1470 m/s for the Yellow Shark environmental model [2]. Compared to that of reference sediment shown in Fig. 1, the frequency shifts of the four striations L1, R1, L2 and R2 are -9.36 Hz, -9.68 Hz, -8.85 Hz and -9.43 Hz, respectively. Using the estimated constant values, the possible sediment parameter perturbations can be found by (5) with err set as 3 Hz. The parameter search space for sediment thickness (in m) is [0.0, 10] with a step of 0.5 m, and for the sediment sound speed (in m/s) is [1440, 1520] with a step of 5 m/s, and the results are shown in Fig. 2. The correct perturbation for the sediment thickness (6 m) and sound speed (10 m/s) is circled in this figure, which is estimated from each individual striation and can be found by a simple structure similar measurement as that in [10].

For numerical simulations, the line structure of the broadband sound distribution can be calculated precisely; therefore the structure similar measurement works well for refinement. While for real data, due to the complexity of the waveguide, unstable passive ship source level and non-flat source spectrogram, the detailed striation structure are usually degraded, not suitable for structure measurement. However, the overall striation slope is preserved well. Here, the Radon transform [14] is employed to extract the striation slope information and then used to refine the preliminary results obtained using the striation location find the best fitting result.

IV. REAL DATA PROCESSING FOR SEDIMENT GEOACOUSTIC CHARACTERIZATION

The MREA/BP'07 sea trial was carried out southeast of the island of Elba in the Mediterranean Sea [15]. Figure 3(a) shows the experiment setup for the passive ship run. R/V Leonardo was used as the noise source of opportunity. The passive acoustic run (red

line) was done near and parallel the Yellow Shark transect [15], R/V Leonardo sailed from SE to NW, and the two compact receiver arrays (shallow and deep) were deployed from a small boat (RHIB) drifting away from the ship course. The sound speed profile (SSP) of the water column used in the forward model is shown in Fig. 3(b), which is measured at the source just before the run.

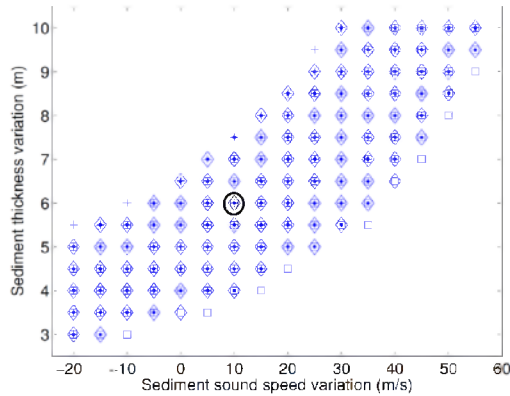


Figure 2: The estimations of the perturbations of sediment layer thickness and sound speed using 5 for both striations, 'point' is for the result from striation L1, 'cross' is the result from striation R1, 'square' is for the result from striation L2, 'diamond' is the result from striation R2.

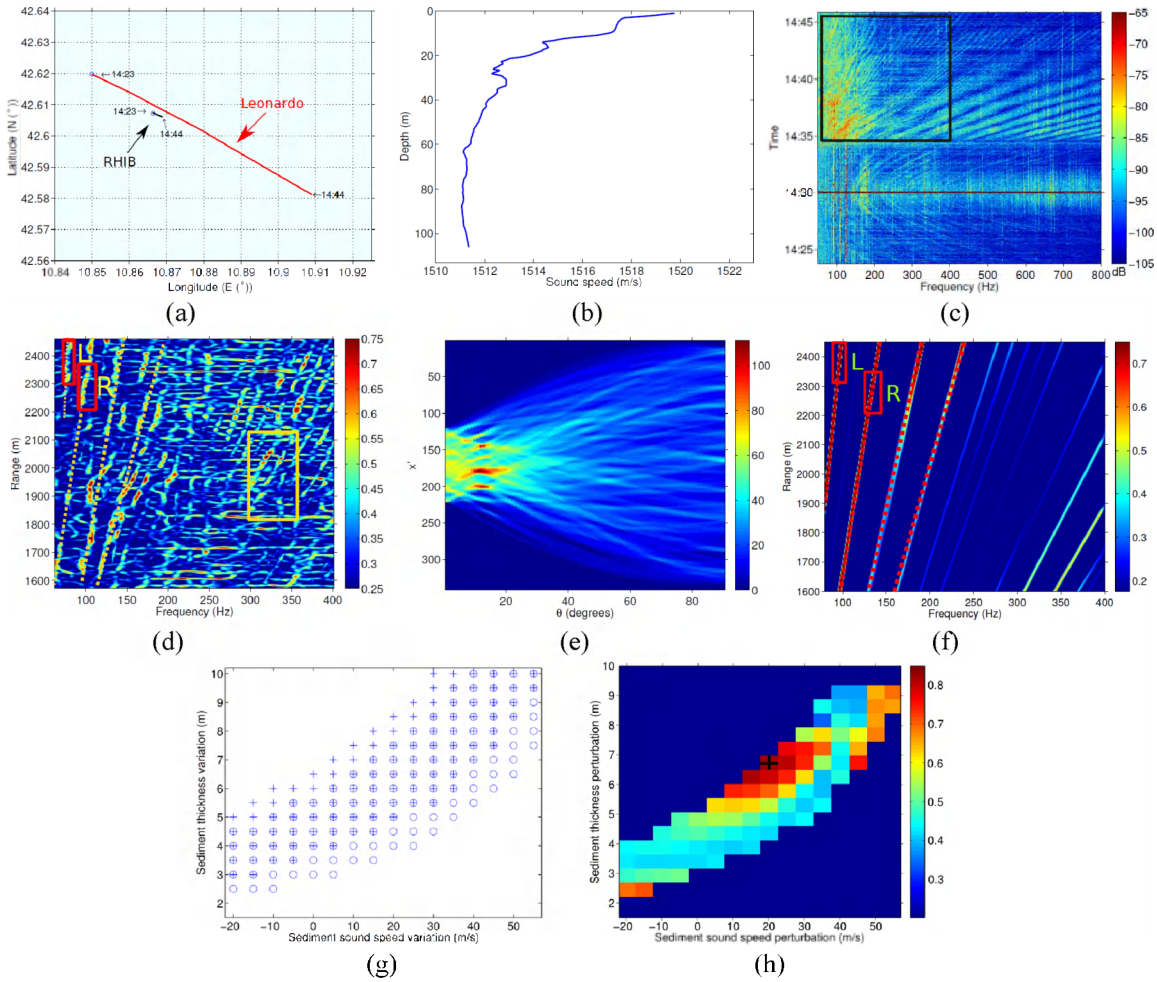


Figure 3. (a) Geometry of MREA/BP07 run L2, 23 April 2007. (b) Sound speed profiles (SSP) taken at R/V Leonardo just before the run. (c) The acoustic pressure spectrogram measured by a single hydrophone. (d) The calculated line structure of the boxed area in Fig. (c). (e) The Radon transform result of the yellow box area in Fig. (d). (f) The interference structure for reference sediment for a 19.6 m depth receiver and corresponding selected striations. (g) The estimations of the perturbations of sediment layer thickness and sound speed for the striations in (d) ('cross' is the results from striation L and 'circle' is the result from striation R). (h) The correlation coefficients between the Radon transform of data and that of possible values.

Figure 3(c) is the spectrogram of the acoustic pressure measured on one hydrophone with an average depth of approximately 19.6 m during the passive acoustic run, which exhibits striations. The horizontal line indicates the closest point of approach (CPA). Due to an abrupt speed change during the navigation, there is an up-shift of the spectral lines in the spectrogram, while the overall structure is well preserved. The boxed area in this figure is analysed for the sediment geoaoustic characterization. Figure 3(d) is the mapped range-frequency spectrogram of the boxed area in Fig. 3(c) after re-sampling along time axis. Two salient striations are boxed in this figure, whose position information are used for the sediment geoaoustic characterization. The Radon transform result of the data are shown in Fig. 3(d), a few peaks that correspond to striation slopes are also visible in this figure. Figure 3(f) is the calculated line structure of the interference structure for the reference sediment. Compared to the striations of the interference structure for reference sediment, their shifts are, respectively, -9.43 Hz and -7.82 Hz.

The average constants are used here for sediment geoaoustic characterization. The precision is also set as 3 Hz when using (13) to obtain the preliminary estimations for the sediment geoaoustic property shown in Fig. 3(g). The correlation coefficients of Radon transform matrix [14] contains the striation slope information are calculated between the possible values with that of real data, and the result is shown in Fig. 3(h). From Fig. 3(h), the perturbations (black cross indicted) for sediment thickness of 7.0 m and sound speed of 20 m/s has the highest correlation coefficient of 0.8275. Consequently, the sediment thickness (7.5 m) and sound speed (1480 m/s) are obtained by a summation of reference values (0.5 m, 1460 m/s) and corresponding perturbations (7.0 m, 20 m/s). The inverted sediment thickness is identical with that of active inversion result [2]. The good consistency of the two parameters demonstrates the accuracy of the proposed method in sediment geoaoustic characterization.

V. CONCLUSION

This paper discussed an acoustic interferometry technique for sediment geoaoustic characterization in Shallow water by processing the broadband noise field generated by a moving ship. Rather than inverting for all the geoaoustic parameters of the sediment as that of MFP technique, the method uses the striation structure to estimate the main geoaoustic parameters that affect the sound propagation in the soft-layered Yellow Shark environmental model. The relation between sediment perturbations and striation location extracted by a multi-scale line filter were numerically studied and interpreted. A synthetic test based on the Yellow Shark environmental model demonstrates the feasibility of using local interference structure for sediment geoaoustic characterization. The real data for passive ship run data are processed for sediment characterization. The inversion results for sediment geoaoustic parameters match well with that of active inversion result in this area, demonstrating the accuracy of the proposed method.

ACKNOWLEDGMENT

Work supported by Office of Naval Research grant N00014-07-1-1069 and National Nature Science Foundation of China grant 50979019. The author Qunyan Ren would like to acknowledge the Belgian National Fund for Scientific Research (FNRS) for supporting the research.

REFERENCES

- [1] E. L. Hamilton, "Geoacoustic modeling of the sea floor," *The Journal of the Acoustical Society of America*, vol. 68, pp. 1313–1340, 1980.
- [2] J.-P. Hermand, "Broad-band geoaoustic inversion in shallow water from waveguide impulse response measurements on a single hydrophone: theory and experimental results". *IEEE Journal of Oceanic Engineering*, vol. 24, no. 1, pp. 41–66, 1999.
- [3] M. D. Collins, "Nonlinear inversion for ocean-bottom properties". *The Journal of the Acoustical Society of America*, vol. 92, no. 5, pp. 2770–2783, 1992.
- [4] S. E. Dosso, M. L. Jeremy, J. M. Ozard, and N. R. Chapman, "Estimation of ocean-bottom properties by matched-field inversion of acoustic field data". *IEEE Journal of Oceanic Engineering*, vol. 18, no. 3, pp. 232–239, 1993.
- [5] N. R. Chapman, S. Chin-Bing, D. King, and R. B. Evans, "Benchmarking geoaoustic inversion methods for range-dependent waveguides". *IEEE Journal of Oceanic Engineering*, vol. 28, no. 3, pp.320–330, 2003.
- [6] J.-P. Hermand, M. Meyer, M. Asch, and M. Berrada, "Adjoint-based acoustic inversion for the physical characterization of a shallow water environment". *The Journal of the Acoustical Society of America*, vol. 119, no. 6, pp. 3860, 2006.
- [7] S. Chuprov, "Interference structure of a sound field in a layered ocean," *Ocean Acoustics, Current State*, pp. 71–91, 1982.
- [8] L. M. Brekhovskikh and Y. P. Lysanov, *Fundamentals of Ocean Acoustics*, 3rd ed. Springer, 2003.
- [9] V. G. Petnikov and V. M. Ku, "Shallow water variability and its manifestation in the interference pattern of sound fields," *AIP Conference Proceedings*, vol. 621, pp. 207–217, 2002.
- [10] Q. Y. Ren and J.-P. Hermand, "A robust passive interferometry technique for sediment geoaoustic characterization, " in *OCEANS '11 MTS/IEEE Kona, Hawaii, USA*, 2011
- [11] Q. Y. Ren, J.-P. Hermand, and S. C. Piao, "Space-Frequency Distribution of the Vector Field of Broad-Band Sound in Shallow Water," in *OCEANS '10 MTS/IEEE Seattle Conference - Innerspace: A Global Responsibility*, 2010.
- [12] J.-P. Hermand, "Broad-band geoaoustic inversion in shallow water from waveguide impulse response measurements on a single hydrophone: theory and experimental results". *IEEE Journal of Oceanic Engineering*, vol. 24, no. 1, pp. 41–66, 1999.
- [13] A. F. Frangi, W. J. Niessen, K. L. Vincken, and M. A. Viergever, "Multiscale vessel enhancement filtering," *Medical Image Computing and computer-Assisted Intervention* MICCAI'98, vol. 1496, pp. 130–137, 1998.
- [14] G. Beylkin, "Discrete radon transform" *IEEE Transactions on Acoustics, Speech and Signal Processing*, vol. 35, no. 2: pp. 163–172, 1987.
- [15] J.-P. Hermand and J.-C. Le Gac, "Subseafloor geoaoustic characterization in the kilohertz regime with a broadband source and a 4-element receiver array". In *Oceans 2008 Quebec City, QC*, pages 1–6, 2008.